Lab On a Chip

Dynamic Article Links ►

Cite this: DOI: 10.1039/c0xx00000x

www.rsc.org/loc

ARTICLE TYPE

# A magnetic cell-based sensor†

**Hua Wang,‡[a,b] Alborz Mahdavi, ‡[c,d] David A. Tirrell[d] and Ali Hajimiri*[a]**

***Received (in XXX, XXX) Xth XXXXXXXXX 20XX, Accepted Xth XXXXXXXXX 20XX***
**DOI: 10.1039/b000000x**

## Electronic Supplementary Information

| | |
|---|---|
| Supplementary Figure 1 | CMOS frequency-shift magnetic sensor |
| Supplementary Figure 2 | Preparation of mouse embryonic stem cells (ESCs) |
| Supplementary Figure 3 | Oscillator line-width compression effect |
| Supplementary Figure 4 | Correlated double counting (CDC) frequency detection for sensor noise cancellation |
| Supplementary Figure 5 | Sensor noise cancellation measurement |

**Supplementary Figure 1 CMOS frequency-shift magnetic sensor**

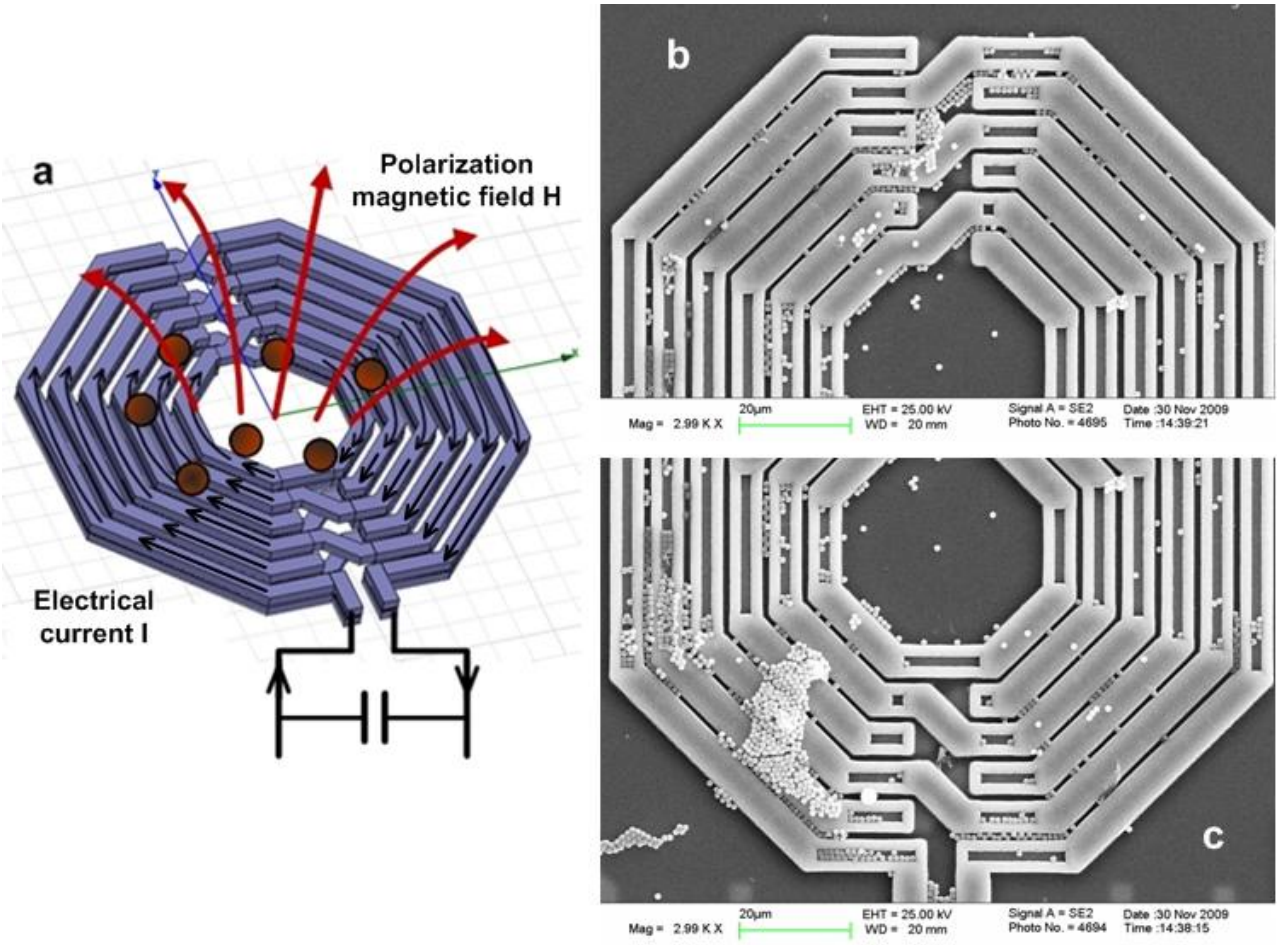


(a) Demonstration of the resonance frequency-shift induced by the magnetic particles. The blue spiral coil represents the sensing inductor, and the brown spheres stand for the magnetic particles. (b) and (c) SEM images of one sensing site with magnetic particles. The outer diameter of the sensor inductor is 120 µm. The grey spheres are magnetic particles with the particle size of 1µm (Invitrogen Dynabeads® MyOne™).

Journal Name

Dynamic Article Links ►

Cite this: DOI: 10.1039/c0xx00000x

www.rsc.org/xxxxxx

ARTICLE TYPE

**Supplementary Figure 2 Preparation of mouse embryonic stem cells (ESCs)**

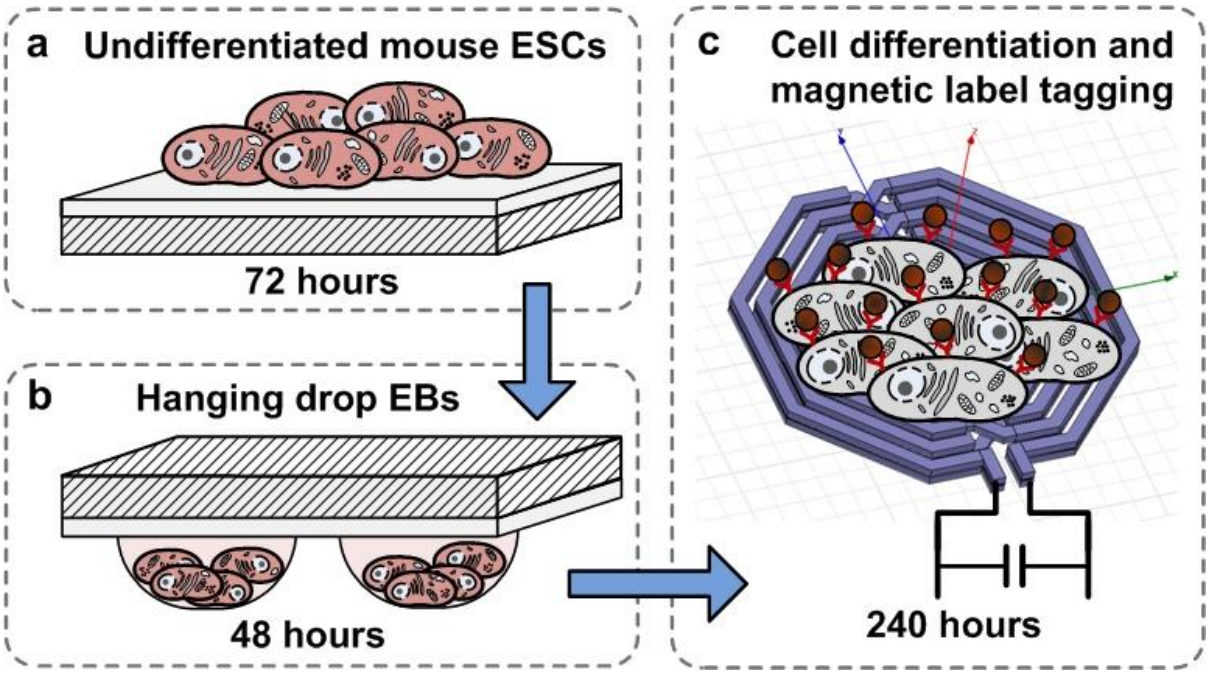


(a) The mouse ESCs were first grown in media with leukemia inhibitory factor (LIF) to maintain their un-differentiated state. (b) We then pre-differentiated the ECS to embryoid bodies (EBs) using the hanging drop technique for 48 hours. (c) The EBs were then seeded onto the sensor surface and grown for additional 10 days in a medium lacking LIF. We achieved reliable cell adhesion to the sensor by coating the CMOS magnetic sensor surface (silicon nitride) with fibronectin ligand.

**Supplementary Figure 3 Oscillator line-width narrowing effect**

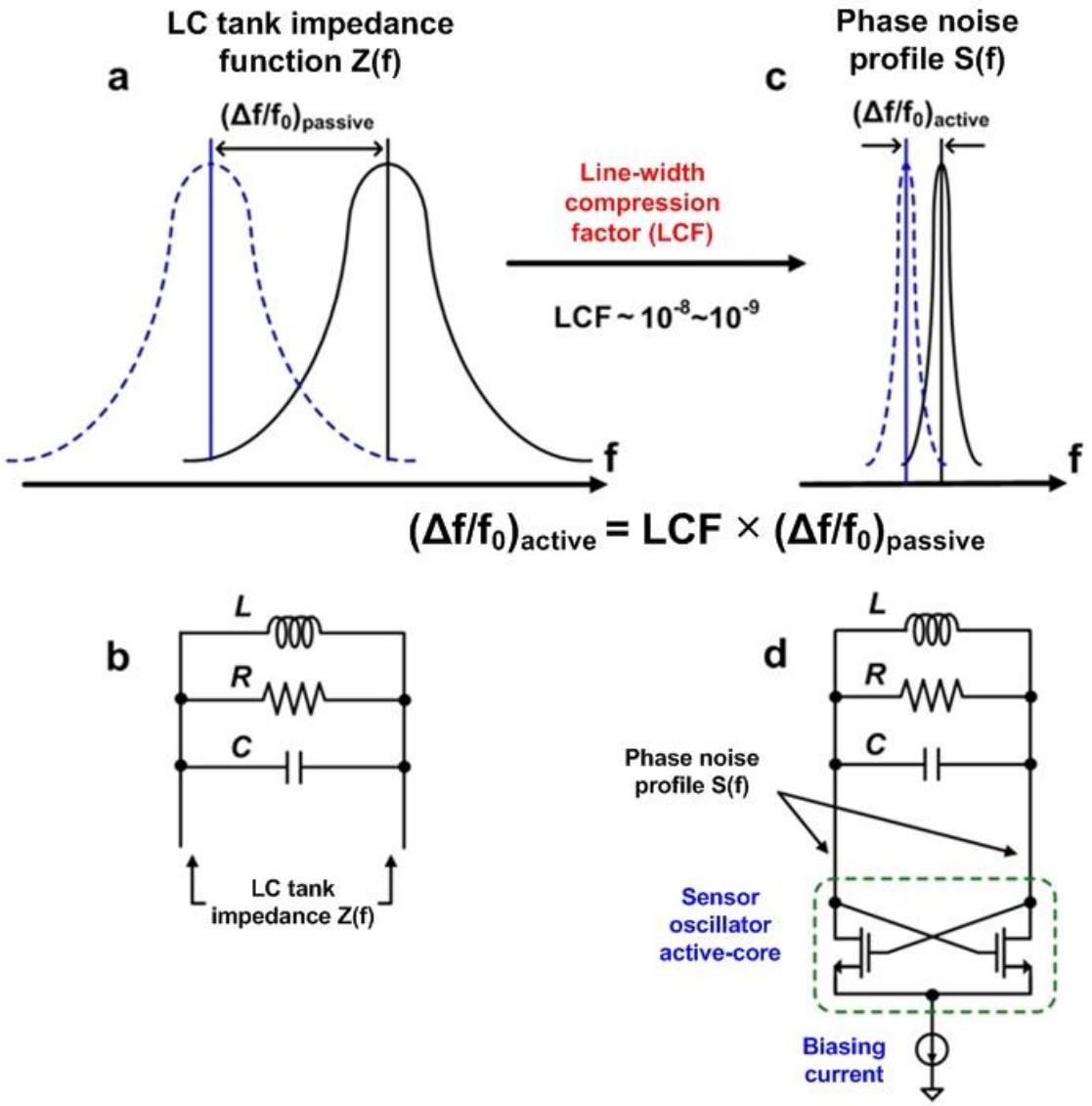


Active oscillator provides an ultrasensitive measurement method to detect the resonance frequency shift in an LC tank due to its line-width compression effect. (a) The impedance function of a lossy parallel LC resonant tank. The widespread impedance function around the resonance frequency results in a poor relative frequency-shift resolution. (b) The equivalent circuit of the parallel LC tank. (c) The phase noise profile of an LC oscillator using the same lossy LC tank as its resonance tank. Compared to the impedance function, the oscillator phase noise profile presents a significant line-width compression effect, which leads to an ultrasensitive frequency-shift resolution[26, 27]. (d) The simplified equivalent circuit of the oscillator with the oscillator active core highlighted.

Journal Name

Dynamic Article Links ►

Cite this: DOI: 10.1039/c0xx00000x

www.rsc.org/xxxxxx

ARTICLE TYPE

**Supplementary Figure 4 Correlated double counting (CDC) frequency detection for sensor noise cancellation**

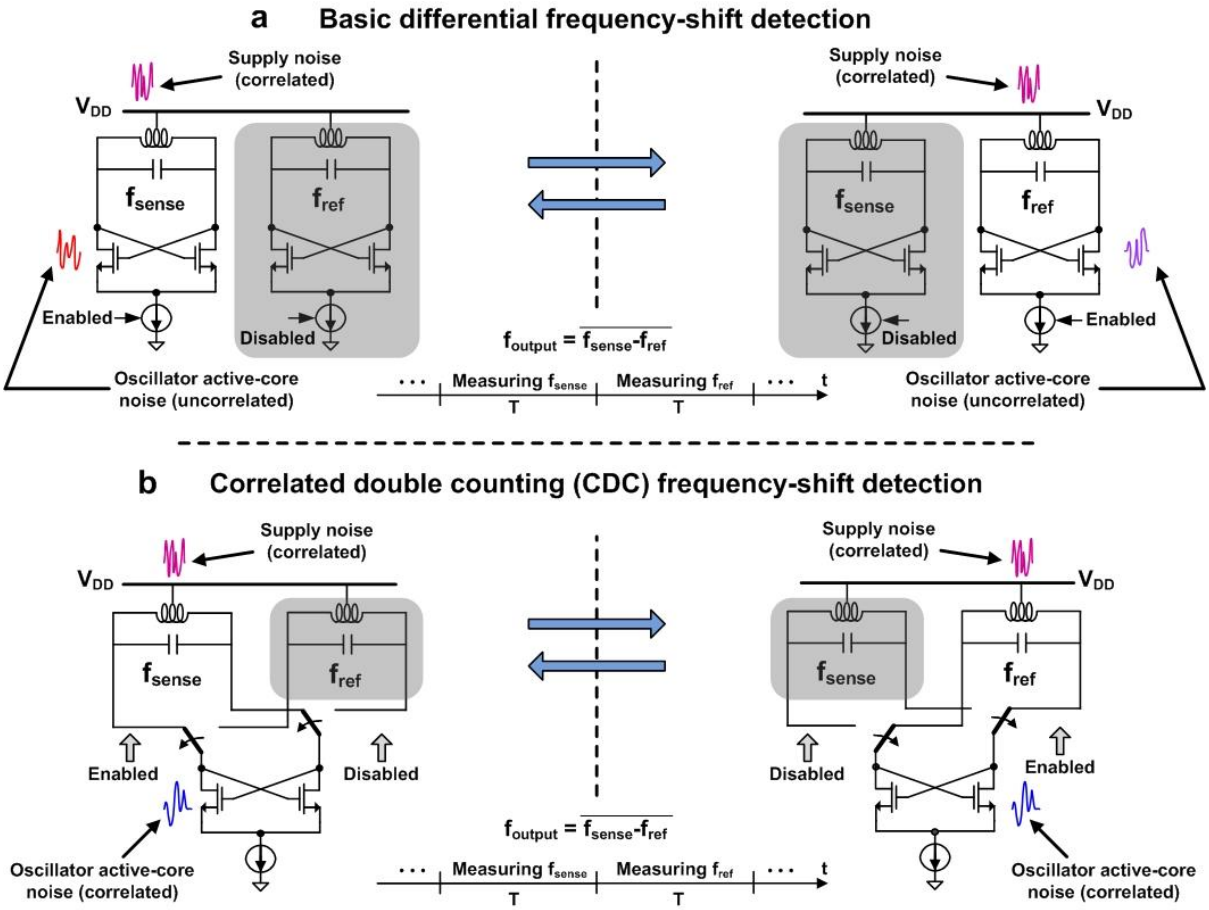


Correlated double counting (CDC) frequency detection further improves the sensitivity of the oscillator-based resonance frequency-shift detection[27]. (a) Basic differential frequency-shift detection. Two sensing oscillators, each with its own LC resonance tank, share the same supply and biasing and are physically adjacent to each other. One sensing oscillator is used as the active sensor and the other as the reference. Thus, environmental noise, e.g. supply noise or temperature variation, is correlated between the two sensors and is suppressed through time-interleaved differential frequency detection by taking the difference of the two sensors' frequency readouts. However, the noise from the oscillator active-core, often as the dominant noise, is uncorrelated and cannot be reduced in the basic differential detection. (b) Correlated double counting (CDC) technique is implemented as two sensing LC tanks (one for actual sensing and the other for reference) sharing the same oscillator active-core. Switching circuits selectively connect one of the sensing tanks to the oscillator active-core. With this CDC technique, the noise from both the environmental perturbations and the oscillator active-core is correlated between the sensing and the reference readouts, and thus is readily to be suppressed through differential operation. For the CMOS magnetic sensor in this work, the CDC scheme is extended to a quad-core configuration with four sensor sites sharing the same oscillator active-core.

**Supplementary Figure 5 Sensor noise cancellation measurement**

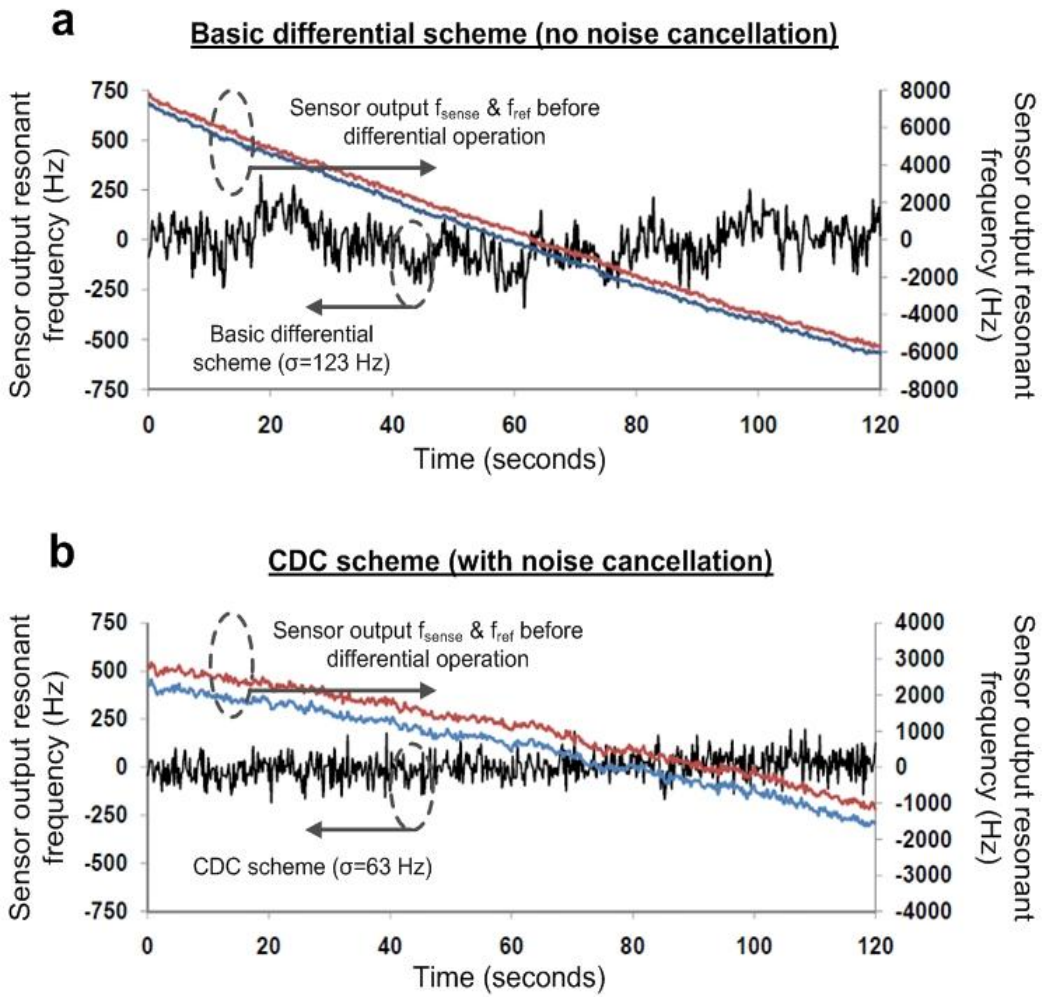


Noise suppression of the CMOS frequency-shift magnetic sensor is demonstrated in a real-time measurement. In both plots, the blue and red curves represent the sensor outputs, as the resonant frequencies, of the active sensor ($f_{sense}$) and the reference sensor ($f_{ref}$), respectively. The black curves show the sensor outputs as the difference between $f_{sense}$ and $f_{ref}$ for the basic differential scheme and the CDC scheme (**Supplementary Fig. 4**). (a) Sensor measurement for the basic differential scheme. There is a slowly-varying common frequency drift for $f_{sense}$ and $f_{ref}$, which is due to the noise from environmental perturbations and significantly degrades the frequency detection capability. With the differential scheme, the common drift is largely removed, which yields a noise floor of 102.1 Hz, i.e. 101.1 ppb (parts-per-billion) at a 1.01 GHz center frequency, for the CMOS frequency-shift magnetic sensor. (b) Sensor measurement for the CDC scheme. With the CDC scheme enabled, noise cancellation is achieved and leads to a noise floor of 63.7 Hz, i.e. 63.1 ppb at a 1.01 GHz center frequency. This is overall 4.1dB noise suppression by the CDC technique in this measurement, which improves the sensitivity. In both plots, a fixed offset of 500 Hz is added to $f_{sense}$ in order to separate the two curves of $f_{sense}$ and $f_{ref}$ for demonstration purpose.